PHYSICAL REVIEW C **95**, 044306 (2017)

Search for the decay of nature's rarest isotope ^{180m}Ta

B. Lehnert,[1,*] M. Hult,[2,†] G. Lutter,[2,‡] and K. Zuber[1,§]
[1]*Institut für Kern- und Teilchenphysik, Technische Universität Dresden, Germany*
[2]*European Commission, JRC-Geel, Retieseweg 111, B-2440 Geel, Belgium*
(Received 13 September 2016; published 6 April 2017)

^{180m}Ta is the rarest naturally occurring quasistable isotope and the longest lived metastable state which is known. Its possible decay via the β^- or the electron capture channel has never been observed. This article presents a search for the decay of ^{180m}Ta with an ultralow background Sandwich HPGe γ spectrometry setup in the HADES underground laboratory. No signal is observed and improved lower partial half-life limits are set with a Bayesian analysis to 5.8×10^{16} yr for the β^- channel and 2.0×10^{17} yr for the electron capture channel (90 % credibility). The total half-life of ^{180m}Ta is longer than 4.5×10^{16} yr. This is more than a factor of two improvement compared to previous searches.

DOI: 10.1103/PhysRevC.95.044306

I. INTRODUCTION

The study of very long living nuclides is by itself a very interesting topic. Considering β decays, this implies highly forbidden transitions. Examples are ^{113}Cd, ^{115}In, and ^{50}V which are fourfold forbidden nonunique decays. Even higher forbidden β decays should exist, for example, in ^{48}Ca and ^{96}Zr which can compete with double β decay.

A very special candidate is ^{180}Ta. From all 300 stable nuclei only nine are odd-odd nuclei and ^{180}Ta is the heaviest one. Furthermore, it is the rarest quasistable isotope of the rare earth elements with an abundance of only 0.01201(8)% [1] and its production in the stellar nucleosynthesis has been debated for decades. The reason for this is that it is bypassed by the main production processes like r and s process (see, for example, [2,3]). Another unique feature of ^{180}Ta is it being the only quasistable isomer as the ground state decays with a half-life of 8.1 h. The ^{180m}Ta is stabilized by its high spin of 9^- due to the spin alignment $\pi_{9/2}[514] + \nu_{9/2}[624]$ while the ground state is antialigned $\pi_{7/2}[404] + \nu_{9/2}[624]$ resulting in a spin of 1^+. Due to the high spin difference, a depopulation of the ^{180m}Ta can only occur by photoexcitation into excited states which have a decay branch into the ground state.

The decay scheme of ^{180m}Ta is shown in Fig. 1. It branches with β decay to ^{180}W and with electron capture (EC) to ^{180}Hf. The lowest spin difference is to the excited 6^+ states which cascade down to the ground states. The transitions would be classified as twofold forbidden unique like, e.g., ^{10}Be, ^{26}Al, ^{138}La, and ^{123}Te β decay.

Several past measurements have been performed to search for the decay of ^{180m}Ta which are summarized in Table I. The best current half-life limits are 4.45×10^{16} yr for the EC branch, 3.65×10^{16} yr for the β^- branch and 2.0×10^{16} yr for the total half-life [13].

The present study is in principle an extension of the previous measurement [13] using the same sample and detectors but incorporates in addition the following features:

(i) 176 more days of measurement time.
(ii) Reduced intrinsic background due to further decay of cosmogenic radionuclides in the sample, detectors, and shield.
(iii) Improved statistical analysis based on spectral fits and calculating the full Bayesian posterior probability.
(iv) Combining multiple γ rays of the de-excitation cascade in a given decay mode.
(v) Combining multiple data sets incorporating all the previous measurements performed in the underground laboratory HADES including the study from 2006 [12] using another tantalum sample.

II. SAMPLE

The natural isotopic abundance of ^{180}Ta is very low and it is very cumbersome and therefore expensive to produce a sample enriched in ^{180m}Ta. Cumming and Alburger [11] used an enriched sample containing 8 mg of ^{180m}Ta, which is relatively small and which has the additional problem of not being perfectly radiopure. For this study, the same sample as in [13] was used which is shown in Fig. 2. This sample consists of six disks with 100 mm diameter and 2 mm thickness of high purity tantalum of natural isotopic composition. The disks have a mass of 1500.33 g translating into a total ^{180m}Ta mass of 180 mg. The disks have been underground in HADES for more than 6 yr prior to these measurements, which guarantees that, e.g., the activity of ^{182}Ta ($T_{1/2} = 114.4$ d) has decreased to insignificant levels and do not disturb these measurements.

III. SETUP

The measurements took place in the laboratory HADES, which is located 225 m underground at the premises of the Belgian Nuclear Research Centre SCK · CEN in Mol, Belgium. In the underground location, the atmospheric μ flux is reduced by a factor 5000 compared to the surface. JRC-Geel operates a range of HPGe detectors in HADES as part of its

*Present address: Physics Department, Carleton University, Ottawa, Canada; bjoern.lehnert@tu-dresden.de
†mikael.hult@ec.europa.eu
‡guillaume.lutter@ec.europa.eu
§zuber@physik.tu-dresden.de

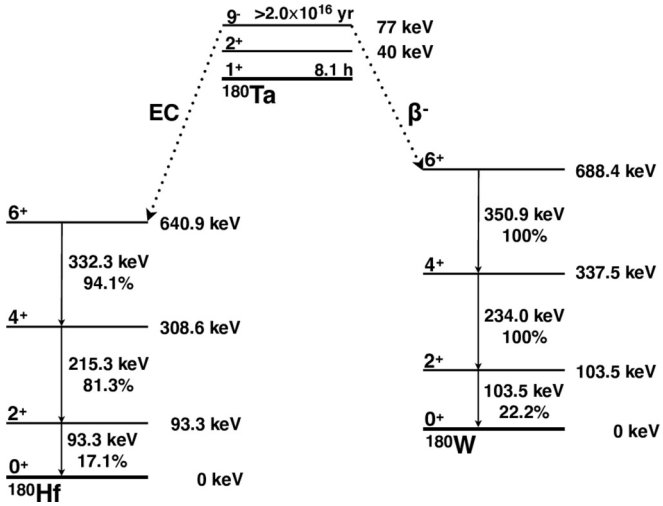

FIG. 1. Decay scheme of ^{180}Ta with data from [4].

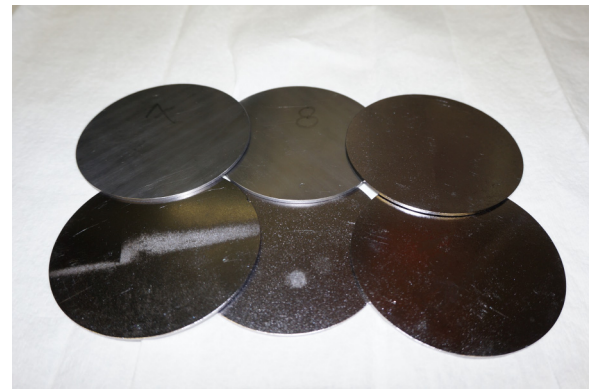

FIG. 2. Picture of the tantalum sample.

radionuclide metrology laboratory. The detectors are used in a wide range of applications stretching from characterization of reference materials and environmental radioactivity studies to measurements of decay data. The shape of the Ta sample makes it highly suitable for measurement in the so-called Sandwich detector system [16]. It consists of two coaxial HPGe detectors, Ge-6 and Ge-7. Detector Ge-6 has a normal U-style arm, while detector Ge-7 has an arm that is rotated 180 deg so that its endcap is facing down. A picture of the arrangement is shown in Fig. 3. Detector Ge-7 was moved downwards so that the distance between the two detector-endcaps was only 1.3 cm for these measurements. Detector Ge-6 has a relative efficiency of 80 % and has a thick (0.5 mm) upper deadlayer, while Ge-7 has a relative efficiency of 90 % and a thin (0.3 μm) upper deadlayer.

An active muon shield made of two plastic scintillator (PS) is installed on the top of the lead shield. The coincidence signal from the two PS is used as a hardware gating signal. This signal and the signals of the two HPGe detectors are sent to standard NIM modules (amplifiers and ADCs) connected to a multiparameter system called DAQ2000 [14]. The DAQ2000 is based on LabView© and designed and manufactured by JRC-Geel. The events are time-stamped with 100 ns binning. All the events are stored in list-mode and the anticoincidence is set by software during the offline analysis. In parallel, the HPGe data are also collected using the Canberra "Genie-2000" acquisition system without muon veto coincidence.

The full energy peak (FEP) efficiencies were calculated using the Monte Carlo code EGSnrc [15]. The two HPGe detectors have been modeled by using physical dimensions provided by manufacturers and extracted from radiographs. The values of the position and the dead layer of the crystal were adjusted until a good agreement (better than 5 %) between the measured and calculated efficiencies was obtained. The Monte Carlo model of the two detectors was also validated through the several participations in proficiency testing schemes. The two decay branches of ^{180m}Ta were simulated separately using the nuclear data from [4]. All γ rays and x rays of the decay scheme were considered so that the calculated FEP efficiencies intrinsically included the coincidence summing effect. Angular correlations were neglected and the simulations assumed that the activity was homogeneously distributed in the sample.

IV. ANALYSIS

The analysis is performed as a spectral fit for the β^- and EC decay mode independently. The fit is performed with

TABLE I. Previous results on ^{180m}Ta half-lives. The various detection techniques are indicated with a simplified description. For measurements [10] and [11] an enriched tantalum sample was used.

Reference	Year	Technique	Lower half-life limit		
			EC	β^-	total
Eberhardt *et al.* [5]	1955	Mass Spec.	—	9.9×10^{11} yr	—
Eberhardt and Signer [6]	1958	Mass Spec.	4.6×10^{9} yr	—	4.5×10^{9} yr
Bauminger and Cohen [7]	1958	γ-spec. NaI	2.3×10^{13} yr	1.7×10^{13} yr	9.7×10^{12} yr
Sakamoto [8]	1967	γ-spec. NaI	1.5×10^{13} yr[a]	—	—
Ardisson [9]	1977	γ-spec. Ge(Li)	2.1×10^{13} yr	—	—
Norman [10]	1981	γ-spec. Ge(Li) enr. Ta	5.6×10^{13} yr	5.6×10^{13} yr	2.8×10^{13} yr
Cumming and Alburger [11]	1985	γ-spec. HPGe enr. Ta	3.0×10^{15} yr	1.9×10^{15} yr	1.2×10^{15} yr
Hult *et al.* [12]	2006	γ-spec. HPGe	1.7×10^{16} yr	1.2×10^{16} yr	7.2×10^{15} yr
Hult *et al.* [13]	2009	γ-spec. Sandwich HPGe	4.45×10^{16} yr	3.65×10^{16} yr	2.0×10^{16} yr

[a]Indication for a positive signal was given.

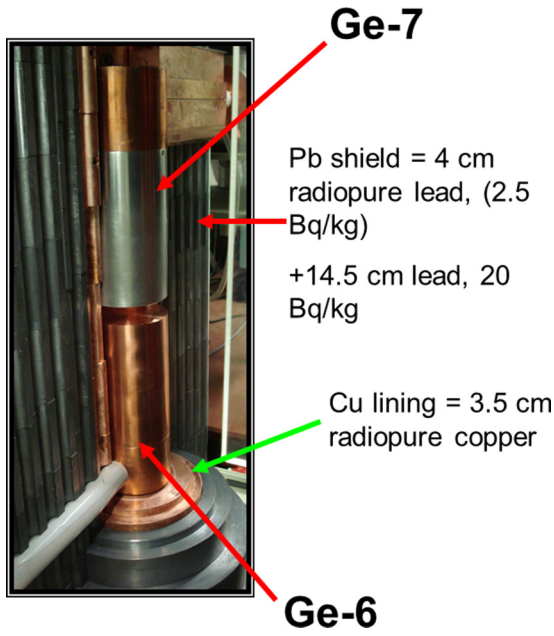

FIG. 3. Picture of the Sandwich spectrometer.

a single half-life parameter on four individual datasets d named "M1" for the 2006 publication [12], "M2" for the 2009 publication [13], and "M3 Ge6" and "M3 Ge7" for the two individual detectors from the recent measurement. The M1 measurement was performed with a single HPGe detector called Ge4 for a live-time of 170 d. The M2 measurement was performed for 68 d with the same sample and Sandwich setup consisting of detectors Ge6 and Ge7 as used for the recent measurement but with their energy spectra combined as shown in Ref. [13]. The M3 measurement was performed for 176 d.

For the β^- branch the single γ line at 234.0 keV is used. The 350.9 keV γ line is omitted because it cannot be clearly distinguished from the prominent 351.9 keV background γ line from ^{214}Pb with the present energy resolution. The 103.5 keV γ line has a small emission probability and small detection efficiency and is thus neglected. For the EC branch also the 93.4 keV γ line is neglected due to the same argument. The fit for this branch is based on the 215.4 keV and 332.3 keV γ lines. Each de-excitation γ line k in a given decay mode has its own fit region of ± 30 keV around the γ line energy. Thus the β^- branch has one fit region and the EC branch has two fit regions.

The signal counts $s_{d,k}$ of each γ line in each dataset are connected with the half-life $T_{1/2}$ of the decay mode as

$$s_{d,k} = \ln 2 \frac{1}{T_{1/2}} \epsilon_{d,k} N_A T_d m f \frac{1}{M} , \quad (1)$$

where $\epsilon_{d,k}$ is the full energy detection efficiency of γ line k in dataset d, N_A is the Avogadro constant, T_d is the live-time of the dataset, m is the mass of the Ta sample, f is the natural isotopic abundance of ^{180}Ta, and M the molar mass of natural tantalum. The Bayesian Analysis Toolkit (BAT) [17] is used to perform a maximum posterior fit combining all four datasets and γ lines for a given decay mode. The likelihood $\mathcal{L}$ is defined as the product of the Poisson probabilities of each bin i in fit region k in every dataset d

$$\mathcal{L}(\mathbf{p}|\mathbf{n}) = \prod_d \prod_k \prod_i \frac{\lambda_{d,k,i}(\mathbf{p})^{n_{d,k,i}}}{n_{d,k,i}!} e^{-\lambda_{d,k,i}(\mathbf{p})} , \quad (2)$$

where $\mathbf{n}$ denotes the data and $\mathbf{p}$ the set of floating parameters. $n_{d,k,i}$ is the measured number of counts and $\lambda_{d,k,i}$ is the expected number of counts in bin i. $\lambda_{d,k,i}$ is taken as the integral of the extended probability density function (p.d.f.) $P_{d,r}$ in this bin

$$\lambda_{d,k,i}(\mathbf{p}) = \int_{\Delta E_{d,k,i}} P_{d,k}(E|\mathbf{p}) dE , \quad (3)$$

where $\Delta E_{d,k,i}$ is the bin width of 0.5 keV. The counts in the fit region are expected from three different types of contributions which are used to construct $P_{d,k}$: (1) a linear background, (2) the Gaussian signal peak, and (3) a number of Gaussian background peaks. The number and type of background peaks depend on the fit region and will be described later. The full expression of $P_{d,k}$ is written as

$$\begin{aligned} P_{d,k}(E|\mathbf{p}) = {} & B_{d,k} + C_{d,k}(E - E_0) \\ & + \frac{s_{d,k}}{\sqrt{2\pi}\sigma_{d,k}} \exp\left(- \frac{(E - E_k)^2}{2\sigma_{d,k}^2} \right) \\ & + \sum_{l_k} \left[\frac{b_{d,l_k}}{\sqrt{2\pi}\sigma_{d,k}} \exp\left(- \frac{\left(E - E_{l_k}\right)^2}{2\sigma_{d,k}^2} \right) \right]. \end{aligned} \quad (4)$$

The first line is describing the linear background with the two parameters $B_{d,k}$ and $C_{d,k}$. The second line is describing the signal peak with the energy resolution $\sigma_{d,k}$ and the γ line energy E_k. The third line is describing the l_k background peaks in fit region k with the strength of the peak b_{d,l_k} and the peak position E_{l_k}. The same p.d.f. with different parameter values is used for all four datasets.

The free parameters $\mathbf{p}$ in the fit for the β^- (EC) branch are:

(i) 1 (1) inverse half-life $(T_{1/2})^{-1}$ with flat prior,
(ii) 8 (16) linear background parameters $B_{d,k}$ and $C_{d,k}$ with flat priors,
(iii) 4 (8) energy resolutions $\sigma_{d,k}$ with Gaussian priors,
(iv) 4 (8) detection efficiencies $\epsilon_{d,k}$ with Gaussian priors,
(v) 1 (2) signal peak positions E_k with Gaussian priors,
(vi) l_1 ($l_1 + l_2$) background peak strength b_{d,l_k} with flat priors,
(vii) l_1 ($l_1 + l_2$) background peak positions E_{l_r} with Gaussian priors.

TABLE II. Energy resolution in FWHM for all γ lines and datasets. The uncertainty is taken as 5 % of the nominal value.

γ line energy	M1	M2	M3_Ge6	M3_Ge7
β^-				
234.0 keV	1.56 keV	1.75 keV	1.82 keV	1.50 keV
EC				
215.3 keV	1.54 keV	1.75 keV	1.80 keV	1.49 keV
332.3 keV	1.63 keV	1.85 keV	1.91 keV	1.57 keV

TABLE III. Full energy peak detection efficiencies per decay of ^{180m}Ta into the β^- or EC branch. The uncertainty on the efficiencies is taken as 10 % of the nominal value.

γ line energy	M1	M2	M3_Ge6	M3_Ge7
β^-				
234.0 keV	0.54 %	1.16 %	0.46 %	0.66 %
EC				
215.3 keV	0.45 %	0.96 %	0.38 %	0.55 %
332.3 keV	1.07 %	2.40 %	0.96 %	1.34 %

The energy resolutions are determined using reference point sources including ^{241}Am, ^{137}Cs, and ^{60}Co. The main γ lines of these radionuclides are fitted by a Gaussian distribution and the calculated energy resolutions are interpolated by a quadratic function. The mean of the Gaussian priors is taken from these calibrations and reported in Table II. The width of these priors is taken as the uncertainty of the resolution calibration curve and approximated with 5 % for all datasets and γ lines.

The full energy peak detection efficiencies as determined with the MC simulations are reported in Table III. These values are taken as the mean value of the Gaussian prior. The uncertainty of the detection efficiencies is approximated with 10 % for each dataset and γ line and used as the width of the prior.

The posterior probability distribution is calculated from the likelihood and prior probabilities with BAT. The maximum of the posterior is the best fit. The posterior is marginalized for $(T_{1/2})^{-1}$ and used to extract the half-life limit with the 90 % quantile. This results in 90 % credibility intervals (C.I.) for the half-life. Systematic uncertainties are included via the width of the Gaussian prior probabilities.

V. RESULTS

The single fit region for the β^- branch is shown in Fig. 4. Two background peaks are considered in the fit region at 238.6 keV coming from ^{212}Pb (43.6 %) and at 241.0 keV coming from ^{224}Ra (4.1 %) where the values in parenthesis denote the emission probability. The best fit is shown as blue line in the plots and finds zero counts for the signal process. The 90 % quantile of the marginalized posterior inverse half-life distribution yields a half-life limit of

$$\beta^- : T_{1/2} > 5.8 \times 10^{16}\ \text{yr (90 \% C.I.)} . \quad (5)$$

This is illustrated in the plots as the red line where the signal peak strength is set to the half-life limit for each dataset.

The background rate underneath the signal peak is determined from the fit as 1.53 cts/keV/d for Ge6 in M3, 1.17 cts/keV/d for Ge7 in M3, 2.99 cts/keV/d for M2, and 2.35 cts/keV/d for M1. The comparison between the Sandwich setup in 2009 with 2.99 cts/keV/d and in 2015 with 2.70 cts/keV/d illustrates the background reduction over time by about 10%, e.g., due to the decay of ^{182}Ta ($T_{1/2} = 114.7$ d). An investigation of the ^{182}Ta peaks at 1189.0 keV and 1221.4 keV found a 4.5 ± 0.5 mBq activity in M2 whereas only a < 0.23 mBq (90% CL) upper limit in M3. Also the background contributions from ^{214}Bi and ^{214}Pb were found to decrease from a weighted average of 3.7 ± 1.2 mBq in M2 to 2.2 ± 1.6 mBq in M3. See also Ref. [18] for more discussion on backgrounds for these detectors.

The two fit regions for the EC branch are shown in Fig. 5. In the second fit region are two prominent background γ lines at 328.0 keV (3.0 %) and 338.32 keV (11.3 %) from ^{228}Ac which are included in the fit. In the first fit region no background γ line is included. The best fit finds zero counts from the signal process which translates into a half-life limit of

$$\text{EC: } T_{1/2} > 2.0 \times 10^{17}\ \text{yr (90 \% C.I.)} . \quad (6)$$

The background rate underneath the two signal peaks of 215.3 keV and 332.3 keV is 1.65 cts/keV/d and 0.95 cts/keV/d for Ge6 in M3, 1.25 cts/keV/d and 0.70 cts/keV/d for Ge7 in M3, 3.28 cts/keV/d and 1.92 cts/keV/d for M2, and 2.42 cts/keV/d and 1.67 cts/keV/d for M1, respectively. Also for this decay mode the background below the peaks decreased by about 10%.

With these partial half-life limits, the total lower half-life limit of ^{180m}Ta is found as

$$^{180m}\text{Ta: } T_{1/2} > 4.5 \times 10^{16}\ \text{yr (90 \% C.I.)} . \quad (7)$$

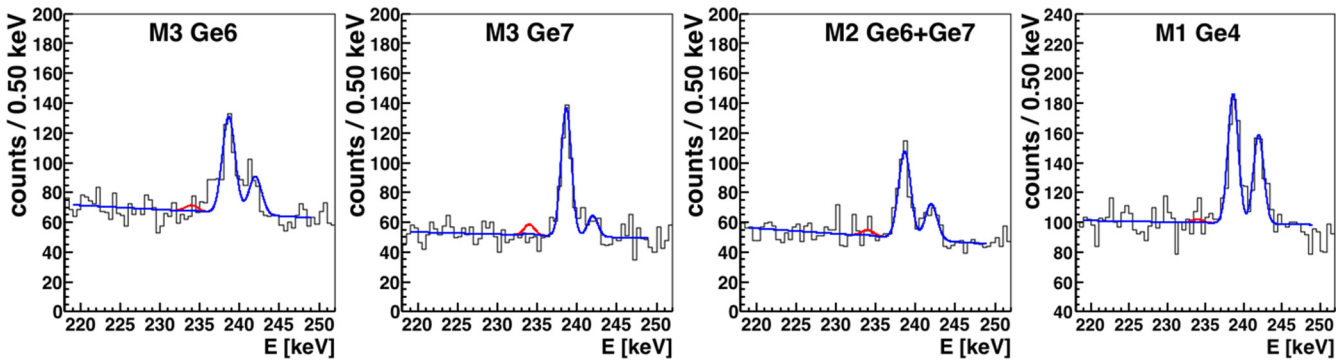

FIG. 4. Region of interest for the β^- channel of ^{180m}Ta decay in the four different datasets. The best fit is shown in blue and the best fit with the signal peak set to the 90 % C.I. half-life limit is shown in red.

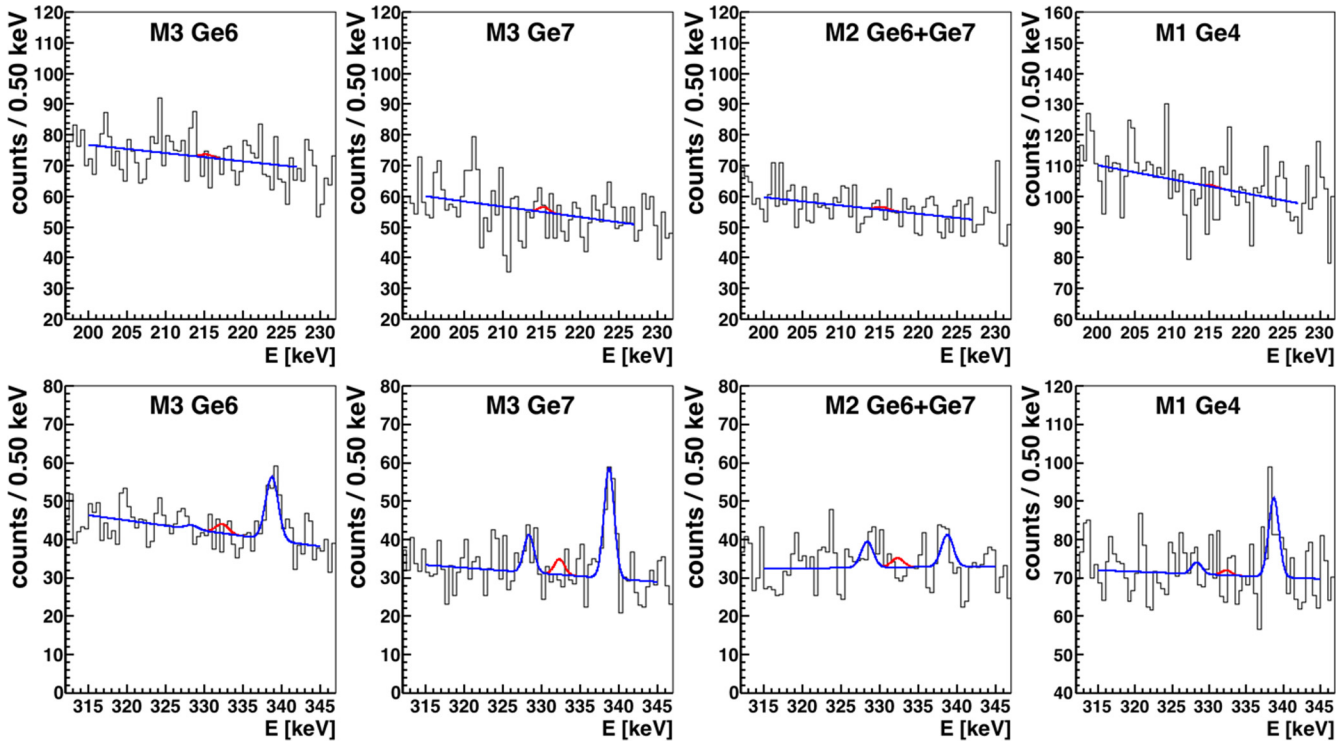

FIG. 5. Regions of interest for the electron capture channel of ^{180m}Ta decay in the four datasets. The best fit is shown in blue and the best fit with the signal peak set to the 90 % C.I. half-life limit is shown in red.

VI. CONCLUSIONS

A new investigation of the β^- decay and EC branch of ^{180m}Ta was performed with a Sandwich HPGe γ spectroscopy setup in the HADES underground laboratory. A significant increase in exposure compared to previous measurements was achieved. In addition, the datasets of the old measurements were combined with the new datasets in a Bayesian framework incorporating various systematic uncertainties. The storage of the sample and the detector system underground for the last years decreased the background for this analysis by about 10% compared to the previous measurement. No signal was observed for either decay mode and a new limit of 5.8×10^{16} yr was set for the β^- branch, 2.0×10^{17} yr for the EC branch and 4.5×10^{16} yr for the total half-life of ^{180m}Ta. Compared to the previously limits, this is an improvement of a factor of 1.6 and 5.5 for the β^- and EC channel, respectively, and an improvement of a factor of 2.3 for the total half-life. The smaller improvement in the β^- channel is mainly due to the fact that the 350.9 keV cannot be effectively used in the spectral fit.

Additional improvements are difficult with this detector system but could be in principle achieved with increasing the target mass in an arrangement which does not decrease the detection efficiency. Further lowering the environmental background in a deeper underground location with more radiopure detector materials would also be beneficial.

ACKNOWLEDGMENTS

This project was granted under the JRC-Geel's transnational access scheme, EUFRAT. The HADES-staff of EURIDICE is gratefully acknowledged for their work.

[1] J. R. de Laeter and N. Bukilic, Phys. Rev. C **72**, 025801 (2005).
[2] P. Mohr, F. Käppeler, and R. Gallino, Phys. Rev. C **75**, 012802 (2007).
[3] T. Hayakawa, P. Mohr, T. Kajino, S. Chiba, and G. J. Mathews, Phys. Rev. C **82**, 058801 (2010).
[4] E. A. McCutchan, Nucl. Data Sheets **126**, 151 (2015).
[5] P. Eberhardt, J. Geiss, C. Lang, W. Herr, and E. Merz, Z. Naturforschg. **10a**, 796 (1955).
[6] P. Eberhardt and P. Signer, Z. Naturforschg A **13**, 1004 (1958).
[7] E. R. Bauminger and S. G. Cohen, Phys. Rev. **110**, 953 (1958).
[8] K. Sakamoto, Nucl. Phys. A **103**, 134 (1967).
[9] G. Ardisson, Radiochem. Radioanal. Lett. **29**, 7 (1977).
[10] E. B. Norman, Phys. Rev. C **24**, 2334 (1981).

[11] J. B. Cumming and D. E. Alburger, Phys. Rev. C **31**, 1494 (1985).
[12] M. Hult, J. Gasparro, G. Marissens, P. Lindahl, U. Watjen, P. N. Johnston, C. Wagemans, and M. Kohler, Phys. Rev. C **74**, 054311 (2006).
[13] M. Hult *et al.*, Appl. Rad. Isot. **67**, 918 (2009).
[14] J. Gonzalez, New features for spectra calculation introduced in the DAQ2000 system, personal communication (unpublished) (2012).
[15] I. Kawrakow, E. Mainegra-Hing, D. W. O. Rogers, F. Tessier, and B. R. B. Walters, the EGSNRC code system: Monte Carlo simulation of electron and photon transport, National Research Council Canada, PIRS-701 (2015).
[16] J. S. E. Wieslander *et al.*, Appl. Rad. Isot. **67**, 731 (2009).
[17] A. Caldwell, D. Kollár, and K. Kröninger, Comput. Phys. Commun. **180**, 2197 (2009).
[18] M. Hult *et al.*, Appl. Rad. Isot. **81**, 103 (2013).